Supporting Information

Red mud based Fe/C nanostructured materials for multi-interface remediation of Cr(VI)-contaminated soil and stabilization

Shiyu Cao[a,b], Jiangshan Li[a,b,*], Jing Nie[a,b,c], Yanbiao Shi[d], Jiaqi Dong[a,b,c], Lizhi Zhang[d], Qiang Xue[a,b]

[a] *State Key Laboratory of Geomechanics and Geotechnical Engineering, Institute of Rock and Soil Mechanics, Chinese Academy of Sciences, Wuhan 430071, China*

[b] *IRSM-CAS/HK PolyU Joint Laboratory on Solid Waste Science, Wuhan 430071, China*

[c] *University of Chinese Academy of Science, Beijing 100049, China*

[d] *School of Environmental Science and Engineering, Shanghai Jiao Tong University, Shanghai 200240, China*

[*] Correspondence E-mail: jsli@whrsm.ac.cn

11 pages, 1 text, 4 tables, 12 figures

CONTENTS

Text S1. Details for experimental section.

Chemicals and materials. Sodium sulfate, 1,5-diphenylcarbazide, 1,10-phenanthroline, and other related chemicals were purchased from Sinopharm Chemical and were of the analytical grades.

Characterizations of the sample. The morphology and element distribution were conducted with a field emission scanning electron microscope (SEM) (Quanta FEG 250, FEI, USA), a transmission electron microscope (TEM, JEM-2100F, Japanese Electronic Optical Co. Ltd, Japan) and the high-angle annular dark field combined with scanning transmission electron microscope (HAADF-STEM, Tecnai F20). DXR Raman Microscope (Thermo, 121 USA) equipped with a 532 nm laser excitation source, powder X-ray diffraction (XRD, Bruker D8 Advance 25, Germany) and X-ray photoelectron spectroscopy (XPS, ESCALAB 250Xi, Thermo Fisher Scientific, USA) were employed to detect the crystal structures and chemical states of samples, respectively. The organic matter content was detected according to Chinese standard NY/T 1121.6-2006 using the potassium dichromate volumetric method.[1]

Theoretical calculations. The calculations of slab models were carried out via spin-polarized density functional theory (DFT) calculations in the Vienna *Ab initio* Simulation Package (VASP 5.4), and the Perdew-Burke-Ernzerhof (PBE) and generalized gradient approximation (GGA) were chosen.[2,3] The convergence criteria for energy and force were set to 10^{-5} eV and 0.02 eV/Å, respectively, and the cutoff energy and K-point mesh were set to 400 eV and 1*1*1, respectively. The isovalue in deformation charge density result was set to be 0.005 a.u.. The adsorption energy was defined as $\Delta E_{ads} = E_{adsorbate/surf} - E_{adsorbate} - E_{surf}$. Among them, $E_{adsorbate/surf}$, $E_{adsorbate}$, and E_{surf} represent the energy of the adsorption complex, the Cr(VI) molecule, and the surface of stabilizer (biochar-supported nanoscale zero-valent iron, nZVI/BC), respectively.

Table S1a. Physicochemical properties of soil.

Soil properties	Values
pH	7.84
Soil conductivity (μS/cm)	84.70
CEC (cmol/kg)	21.48
Organic matter (g/kg)	4.30

Table S1b. Compositions of red mud.

Composition	Concentration (mg/kg)
Cu	12.20
Zn	108.00
Cd	0.15
Pb	17.40
Cr	10.40
Cr(VI)	9.20
Hg	0.00011
Be	0.18
Ba	88.70
Ni	11.70
Ag	0.079
As	0.00056
Se	0.15

Table S2. Fitting results of Fe 2p HR-XPS spectra in **Figure 2g**.

Samples	Fe(III)	Fe(II)	Fe(0)
Straw	0	0	0
Red mud	58%	42%	0
nZVI/BC	39%	45%	16%

Table S3. TCLP leaching concentrations of possible toxic composition in soil amended by nZVI/BC, and the GB/T5085.3-2007 standard.[4]

Composition	Leaching concentration (mg/L)	Standard (mg/L)
Cu	< 0.00008	100
Zn	< 0.00067	100
Cd	< 0.00005	1
Pb	< 0.00009	5
Cr	11.26	15
Cr(VI)	3.13	5
Hg	< 0.00004	0.1
Be	< 0.00004	0.02
Ba	1.15	100
Ni	0.051	5
Ag	< 0.00002	5
As	< 0.00012	5
Se	< 0.00041	1

Table S4. The summary of chromium presence on nZVI/BC surface and Cr(VI)-contaminated soil (CrSoil) surface after soil remediation.

Cr	Out	MM	BB	Cr(III)
nZVI/BC	0	0	15%	79%
CrSoil	1%	0	5%	0

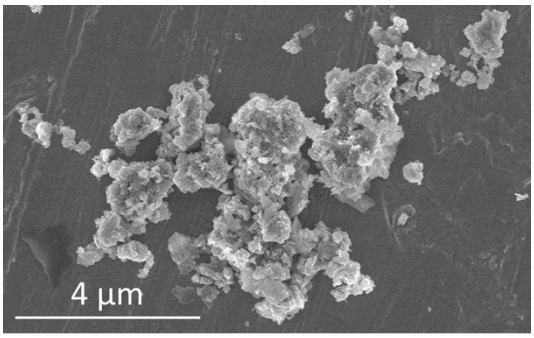

Figure S1. SEM image of nZVI/BC.

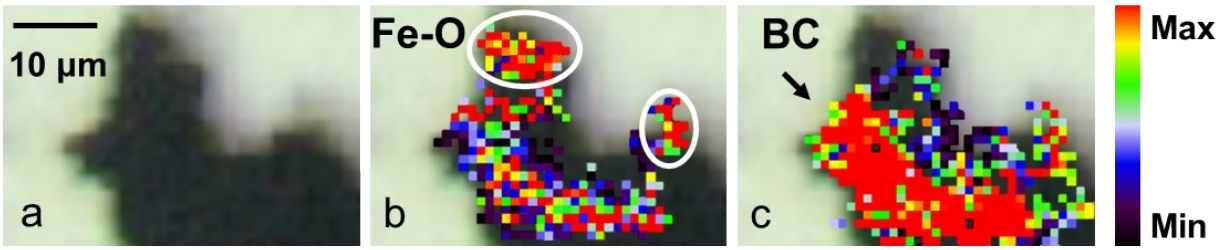

Figure S2. Raman mapping of nZVI/BC. (a) Microscopic images. (b) Intensity distribution of peaks between 800 and 100 cm^{-1}. (c) Intensity distribution of peaks between 2000 and 800 cm^{-1}.[5,6]

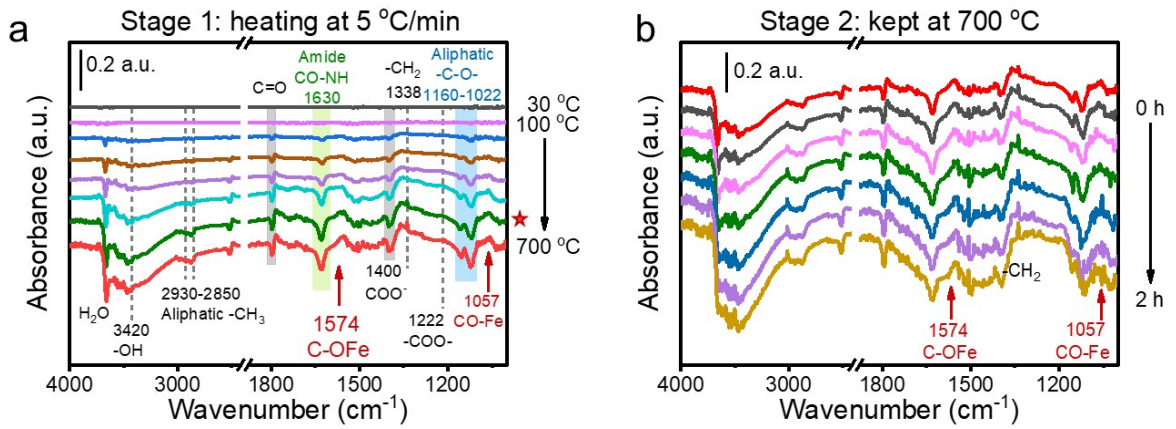

Figure S3. *In situ* DRIFTS spectra during the synthesis of nZVI/BC. (a) The heating process (Stage 1) and (b) the subsequent temperature-keeping process (Stage 2).

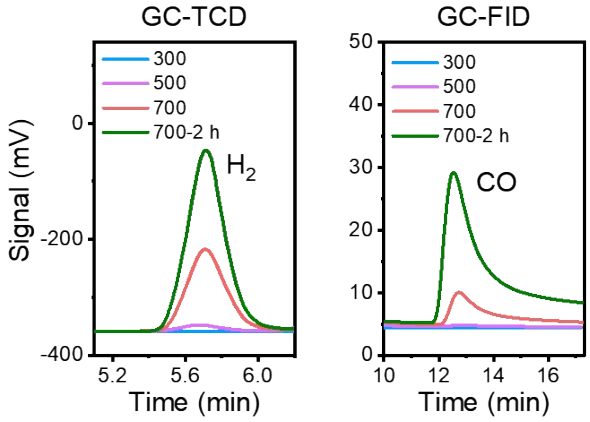

Figure S4. Gas chromatograph (GC) signals during the synthesis of nZVI/BC.

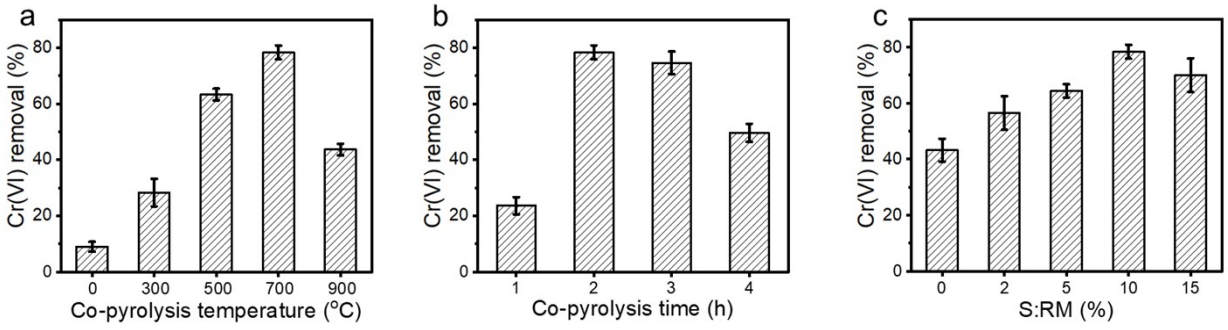

Figure S5. The effect of (a) co-pyrolysis temperature, (b) co-pyrolysis time, and (c) straw dosages on Cr(VI) removal with nZVI/BC. The initial Cr(VI) concentration and material dosage were 4 mg/L and 0.4 g/L, respectively.

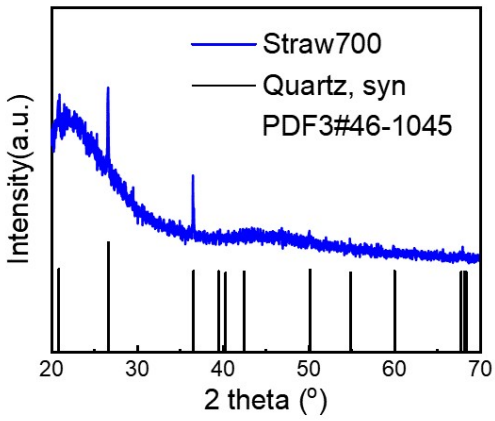

Figure S6. XRD of the Straw700 sample.

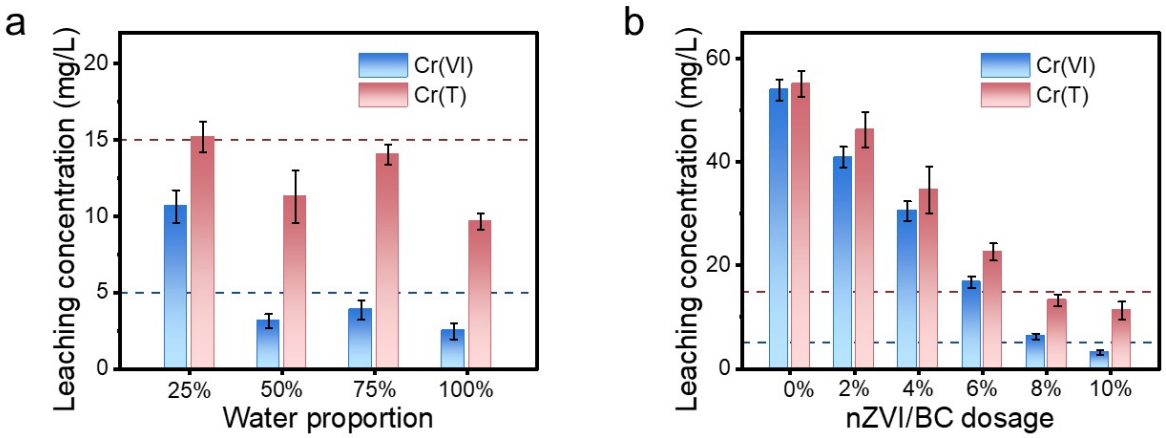

Figure S7. Effect of (a) water proportion and (b) nZVI/BC dosage on Toxicity Characteristic Leaching Procedure (TCLP) leaching properties of Cr(VI) and Cr(T) during Cr(VI) stabilization in soil.

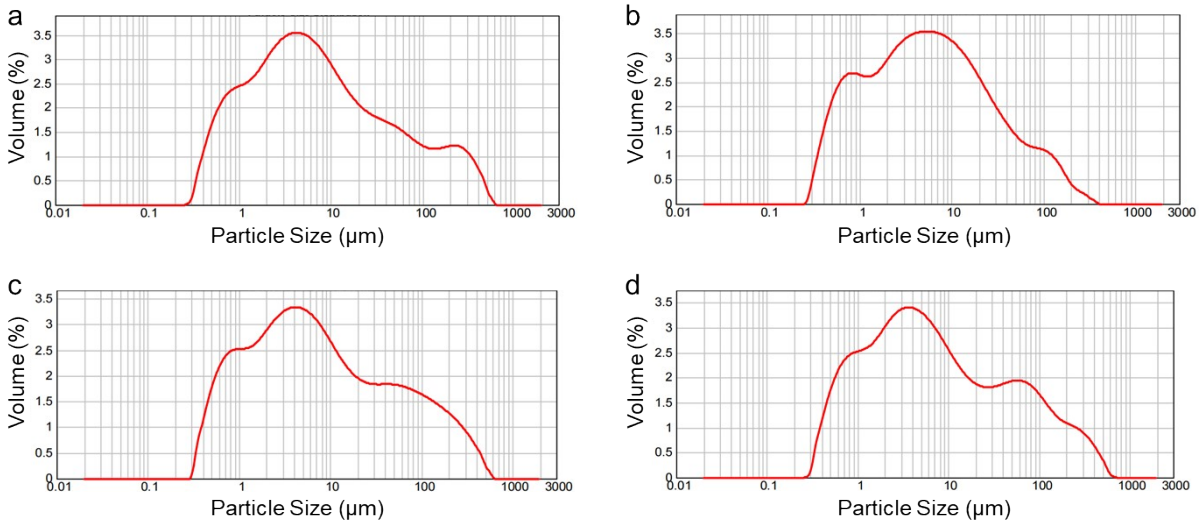

Figure S8. Size distribution of soil particles. (a) Soil, (b) CrSoil, (c) CrSoil remediation by RM700, and (d) CrSoil remediation by nZVI/BC.

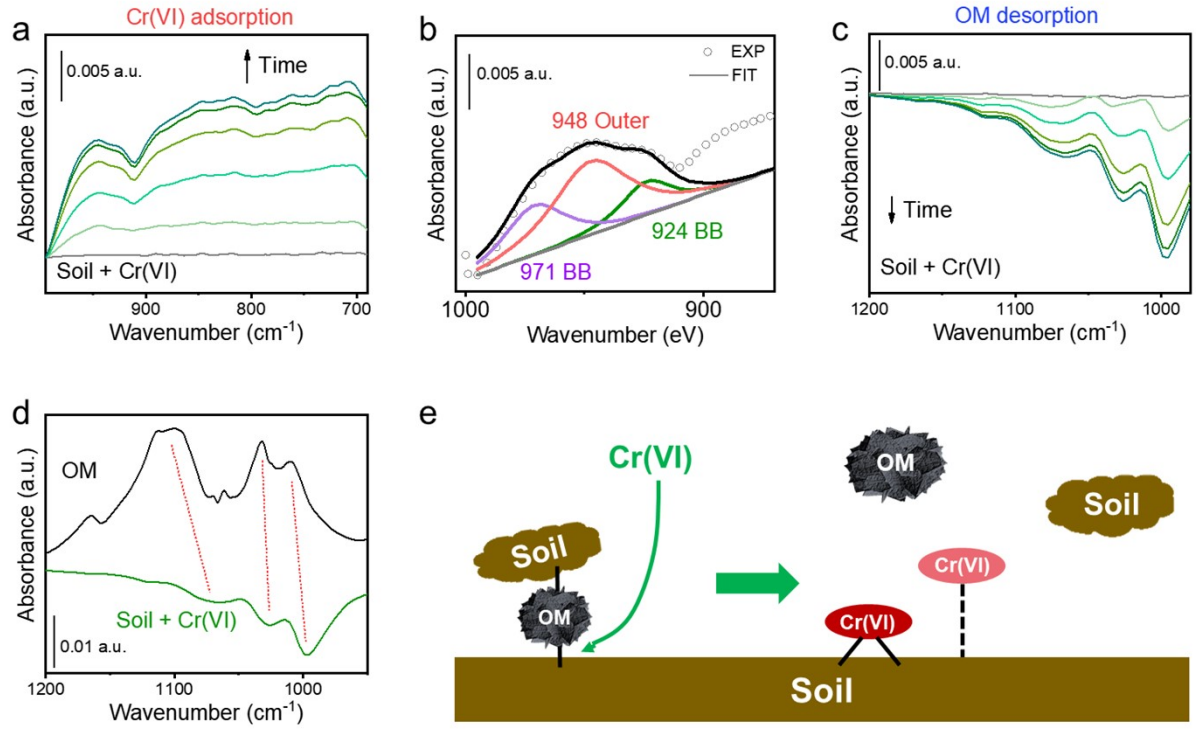

Figure S9. The characterization and mechanism of soil contamination by Cr(VI). (a-c) *In situ* attenuated total reflectance Fourier transform infrared (ATR-FTIR) spectroscopy during soil contaminated by Cr(VI). (d) The infrared spectroscopy of CrSoil and organic matter (OM). (e) Schematic diagram of soil contamination by Cr(VI).

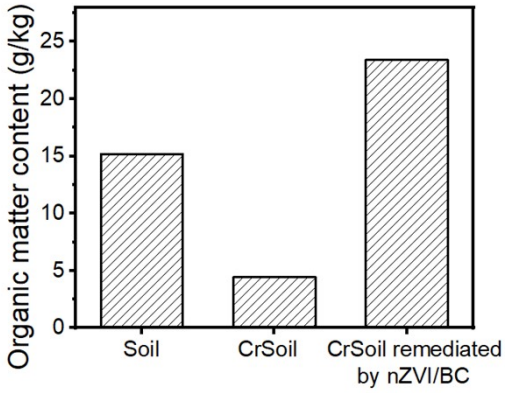

Figure S10. OM content of different soil samples.

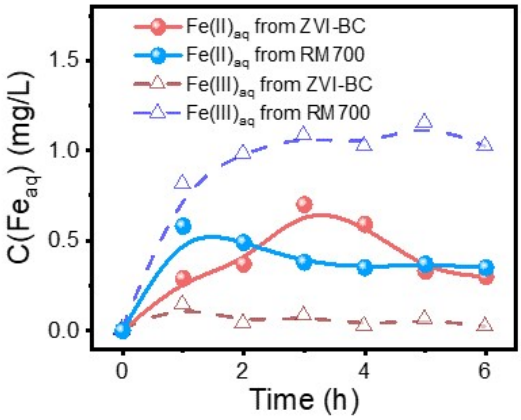

Figure S11. Iron ions released from nZVI/BC and RM700 samples during soil remediation. Initial: 2 g CrSoil, 0.2 g sample, 500 mL water.

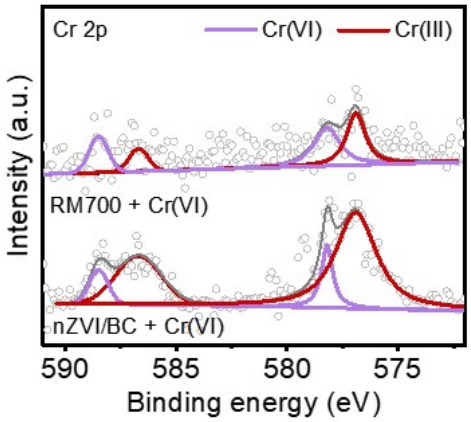

Figure S12. Cr 2p HR-XPS of remediated CrSoil by nZVI/BC and RM700.

References

1 Ministry of Agriculture of the People's Republic of China, Soil Testing Part 6: Method for determination of soil organic matter (NYT1121.6—2006). In China, 2007.

2 W. He, J. Zhang, S.Dieckhöfer, S.Varhade, A. C. Brix, A. Lielpetere, S. Seisel, J. R. Junqueira and W. Schuhmann, Splicing the active phases of copper/cobalt-based catalysts achieves high-rate tandem electroreduction of nitrate to ammonia, *Nat. Commun.*, 2022, **13**, 1129.

3 T. Ohmori, M. S. El-Deab and M. Osawa, Electroreduction of nitrate ion to nitrite and ammonia on a gold electrode in acidic and basic sodium and cesium nitrate solutions. *J. Electroanal. Chem.,* 1999, **470**, 46-52.

4 China Ministry of Ecology and Environment, Identification standards for hazardous wastes-Identification for extraction toxicity (GB 5085.3—2007). In China, 2007.

5 S. Cao, G. Zhan, K. Wei, B. Zhou, H. Zhang, T. Gao and L. Zhang, Raman spectroscopic and microscopic monitoring of on-site and in-situ remediation dynamics in petroleum contaminated soil and groundwater, *Water Res.*, 2023, **233**, 119777.

6 S. Cao, X. Zhang, X. Huang, S. Wan, X. An, F. Jia and L. Zhang, Insights into the facet-dependent adsorption of phenylarsonic acid on hematite nanocrystals, *Environ. Sci.: Nano*, 2019, **6**, 3280-3291.